AD-A122 034 A TECHNIQUE FOR PREDICTING SURFACE WIND DISTRIBUTIONS OF TROPICAL CYCLONE..(U) NAVAL ENVIRONMENTAL PREDICTION RESEARCH FACILITY MONTEREY CA.. T L TSUI ET AL. OCT 82 1/1

UNCLASSIFIED NEPRF-TR-82-05 F/G 4/2 NL

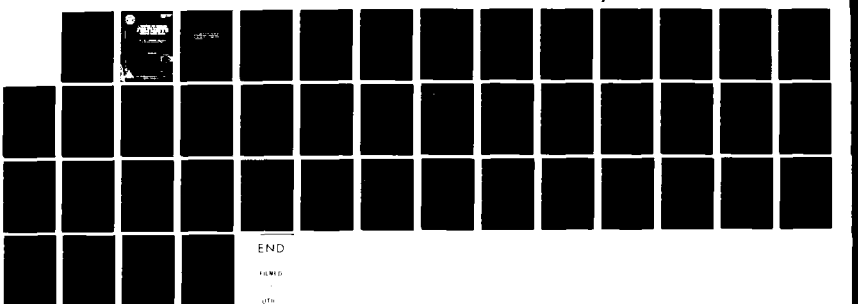

END

FILMED

DTIC

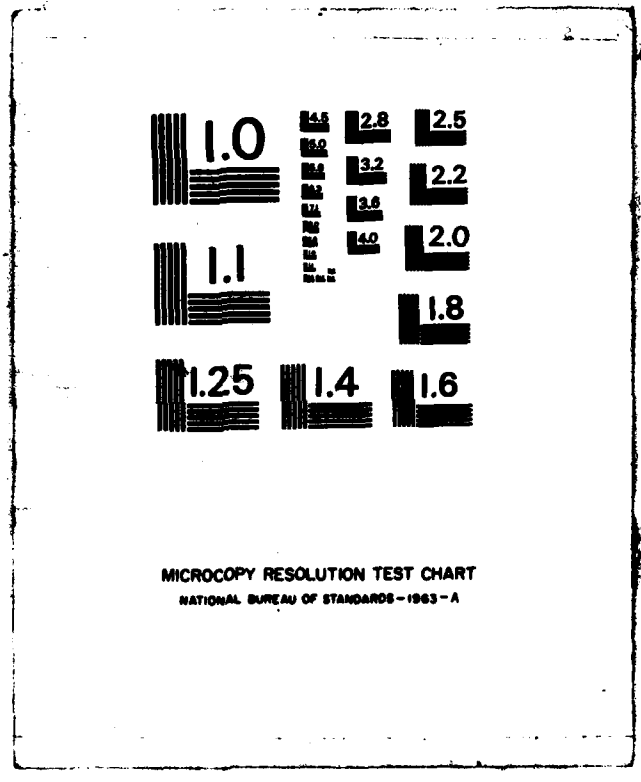
1.0
1.1
1.25
1.4
1.6
2.8
3.2
3.6
4.0
5.0
2.5
2.2
2.0
1.8
MICROCOPY RESOLUTION TEST CHART
NATIONAL BUREAU OF STANDARDS-1963-A

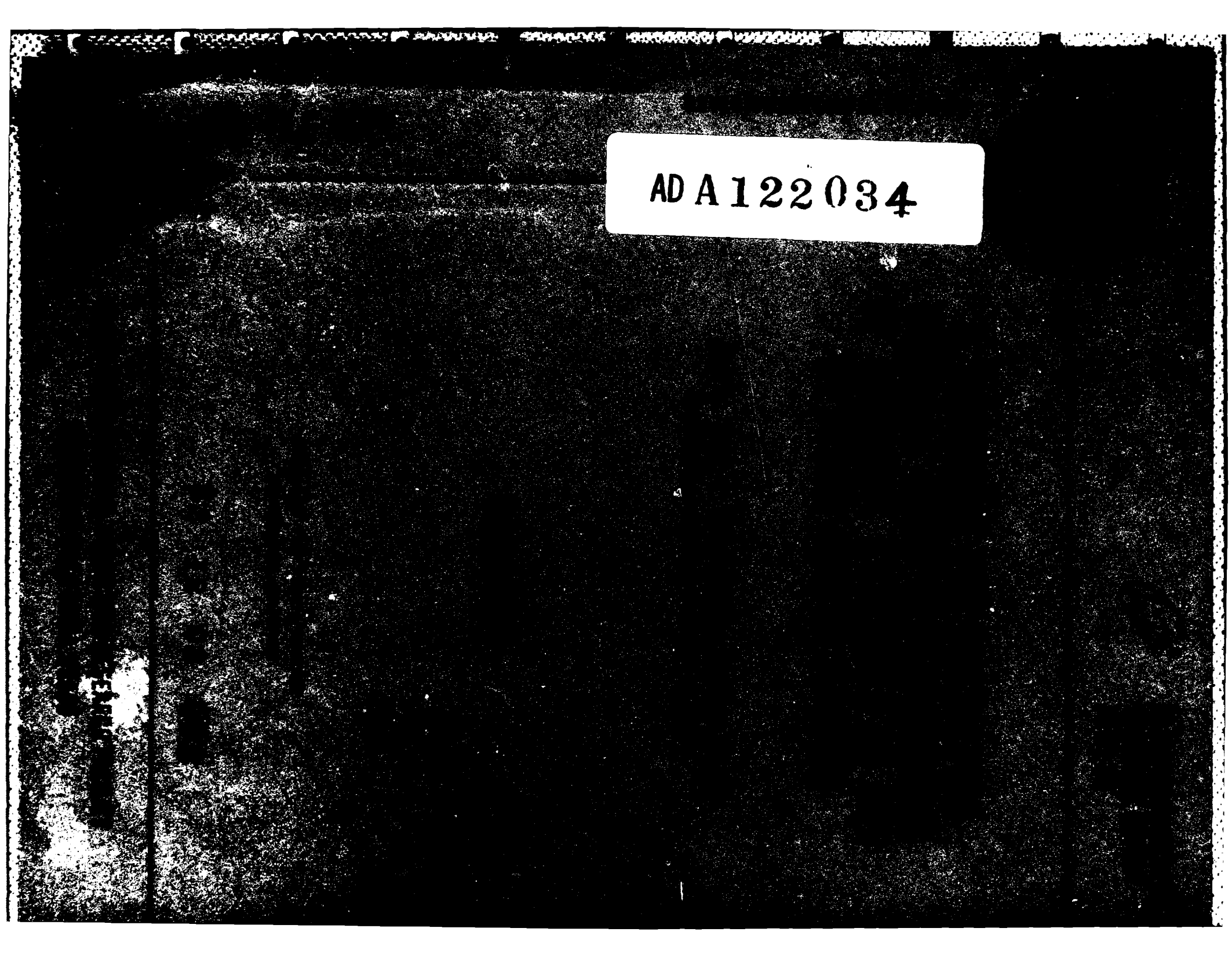

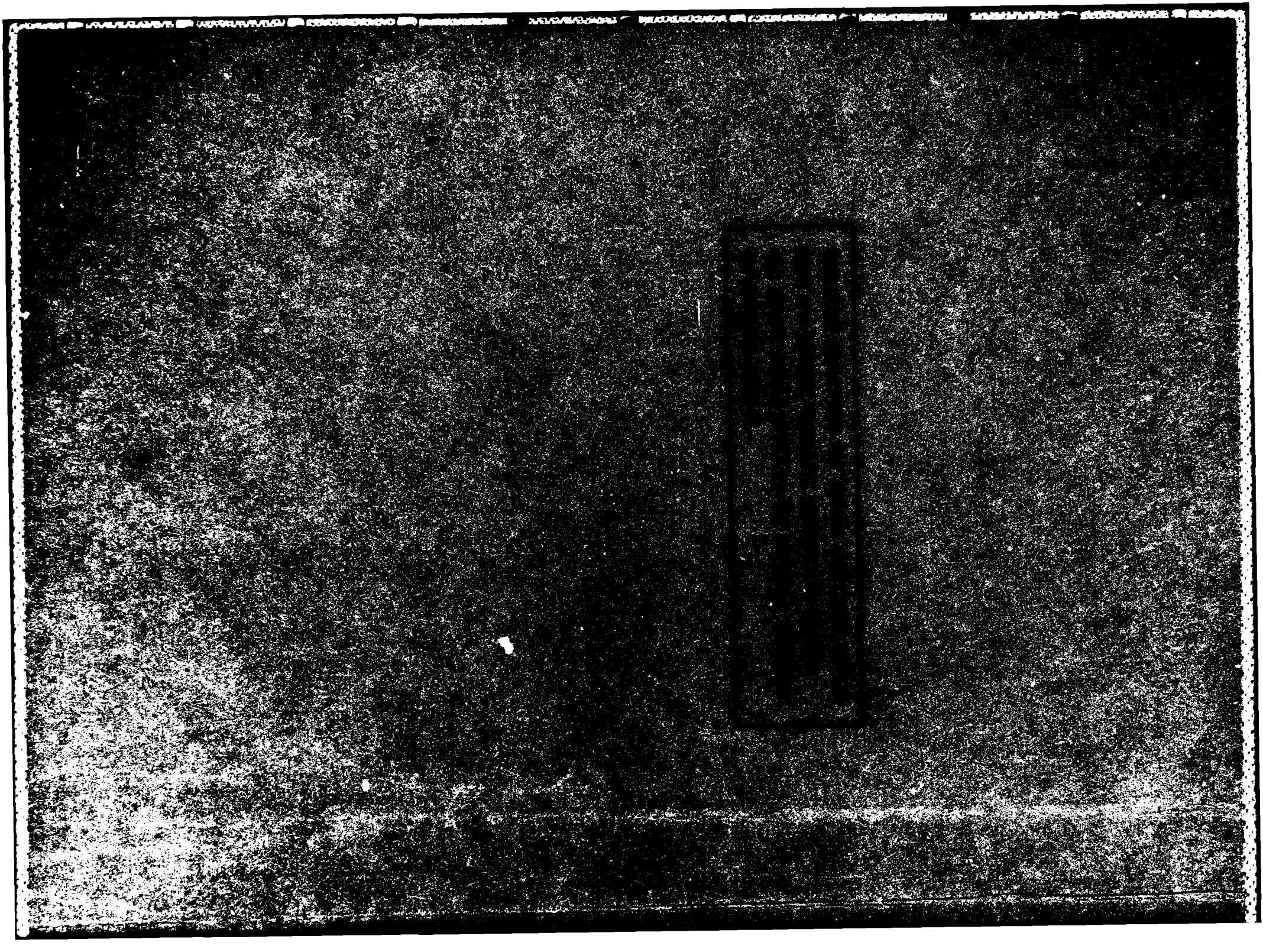

UNCLASSIFIED

SECURITY CLASSIFICATION OF THIS PAGE (When Data Entered)

REPORT DOCUMENTATION PAGE		READ INSTRUCTIONS BEFORE COMPLETING FORM
1. REPORT NUMBER NAVENVPREDRSCHFAC Technical Report TR 82-05	2. GOVT ACCESSION NO. AD-A122034	3. RECIPIENT'S CATALOG NUMBER
4. TITLE (and Subtitle) A Technique for Predicting Surface Wind Distributions of Tropical Cyclones in the Western North Pacific		5. TYPE OF REPORT & PERIOD COVERED Final
		6. PERFORMING ORG. REPORT NUMBER TR 82-05
7. AUTHOR(s) Ted L. Tsui, L. Robin Brody, Samson Brand		8. CONTRACT OR GRANT NUMBER(s)
9. PERFORMING ORGANIZATION NAME AND ADDRESS Naval Environmental Prediction Research Facility Monterey, CA 93940		10. PROGRAM ELEMENT, PROJECT, TASK AREA & WORK UNIT NUMBERS PE 63207N PN 7W0513 TA CC00 NEPRF WU 6.3-2
11. CONTROLLING OFFICE NAME AND ADDRESS Naval Air Systems Command Department of the Navy Washington, DC 20361		12. REPORT DATE October 1982
		13. NUMBER OF PAGES 42
14. MONITORING AGENCY NAME & ADDRESS(if different from Controlling Office)		15. SECURITY CLASS. (of this report) UNCLASSIFIED
		15a. DECLASSIFICATION/DOWNGRADING SCHEDULE

16. DISTRIBUTION STATEMENT (of this Report)

Approved for public release; distribution unlimited.

17. DISTRIBUTION STATEMENT (of the abstract entered in Block 20, if different from Report)

18. SUPPLEMENTARY NOTES

19. KEY WORDS (Continue on reverse side if necessary and identify by block number)

Tropical cyclone wind distribution
Tropical cyclone forecasting
Statistical forecasting

20. ABSTRACT (Continue on reverse side if necessary and identify by block number)

Accurate initial estimates and forecasts of radii of winds over 30 kt and 50 kt around tropical cyclones are important requirements for Navy decision-making and operations. This report describes a diagnostic study of tropical cyclone surface wind distribution that was conducted by using data extracted from tropical cyclone warnings issued by the Joint Typhoon Warning Center, Guam, during the period 1966-77.

((Continued on reverse))

DD FORM 1 JAN 73 1473 EDITION OF 1 NOV 65 IS OBSOLETE S/N 0102-014-6601 |

UNCLASSIFIED

SECURITY CLASSIFICATION OF THIS PAGE (When Data Entered)

Block 20, Abstract, continued.

Results from two different data analyses show that: (1) The tangential wind speed along the radial axis decreases exponentially outward from the radius of maximum wind; (2) In addition to persistence, the change of a tropical cyclone's size depends only on the change of the maximum wind; and (3) The assymetric shape of the isotachs correlates highly to the speed of movement.

Based on these findings, a statistical wind-radius forecast model was formulated and tested on independent 1979 data. Results show that a time lag exists between the change of maximum wind and the change of wind radii, which suggests that the wind-pressure gradient adjustments may originate from the inner core of the storm and slowly propagate outward. The results also indicate that the statistical forecast model possesses a skill equal to that of an average JTWC forecaster's wind radius forecast.

CONTENTS

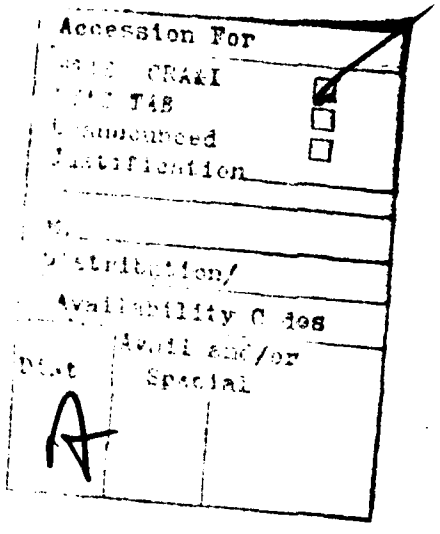

1. BACKGROUND

The success of a Navy operation could well depend upon accurate forecasts of the hazardous sea conditions which are often generated by the surface winds of an approaching tropical cyclone. Appropriate evasive actions could ensure the safety of fleet units and reduce storm damage to a minimum.

An important forecasting task of the Joint Typhoon Warning Center (JTWC) on Guam is the issuing of radius forecasts for the winds over 30, 50, and 100 kt around tropical cyclones. Despite the importance of these wind radius forecasts, very few diagnostic or prognostic studies of them have been made because of the scarcity of observed data. This present study has a twofold intent: (1) to deduce a typical surface wind distribution around a western North Pacific tropical cyclone; and (2) to develop objective forecast aids to predict the tropical cyclone surface wind distributions.

The existence of an organized wind distribution near the surface around a tropical cyclone was suggested first by Byers (1944) and Deppermann (1947). Deppermann used data collected from typhoons near the Philippines and proposed that the surface wind distribution profile outside of the eye wall of the tropical cyclone could be approximated by a Rankine Vortex. In consideration of the momentum loss caused by surface friction, Hughes (1952) and Riehl (1963) modified the Rankine Vortex wind profile to,

$$vr^{\alpha} = \text{const}, \qquad (1)$$

where v is the tangential wind speed, r the radius and $\alpha \approx 0.55$, the empirically determined constant for the winds at gradient level (~900 mb). Shea and Gray (1973) used the data compositing technique and showed that α can vary from storm to storm. Sheets (1978) applied the above wind radius relationship to data collected by NOAA P-3 research aircraft during penetrations of Atlantic Hurricane Anita (1977), and found α varying from 0.2 to 0.7.

Using a gradient wind relationship to describe the wind distribution around a tropical cyclone, Holland (1980) pointed out that shape and scale parameters had to be estimated to use his analytical model in an operational environment. This involved the estimation of the maximum wind (V_{max}), which could be accomplished by using the Atkinson and Holliday (1977) method or the Dvorak (1975) method, and the estimation of the radius of the maximum wind which relied on some climatological relationship.

The results of these several studies were difficult for the Navy to use, since most of the tropical cyclone wind distributions dealt with gradient level winds. In general, surface winds were derived by extrapolation from gradient level winds by using the climatological relationship suggested by Bates (1977). In addition, study results were based on the data collected from Atlantic tropical cyclones whose wind distribution may be different from that of the western North Pacific tropical cyclones.

This present study seeks to circumvent data scarcity problems and to produce and forecast a realistic asymmetric surface wind distribution around a western North Pacific tropical cyclone

2. DISCUSSION OF DATA SOURCES

Possible data sources for surface winds around a tropical cyclone of the western North Pacific region are land, ship and aircraft observations. Land stations can provide accurate wind data from approaching storms, but these wind reports are often biased by local geography/topography; furthermore, few tropical cyclones come close to land. Shipboard observations of strong surface winds over 30 kt around tropical cyclones on the open sea obviously are rare. Surface wind estimates obtained by reconnaissance aircraft during storm penetrations, in fact, are the only data sets that regularly provide wind records.

At JTWC, information on tropical cyclone surface winds comes mainly from these reconnaissance reports. During aircraft penetration, the weather officer aboard continuously converts sea conditions to surface wind speeds on the Beaufort wind scale. Under most conditions, JTWC forecasters are able to acquire detailed descriptions of surface wind conditions via radio link with the weather officer on the aircraft; forecasters generally obtain this wind information about three hours before the warning time. Given all available wind reports, forecasters analyze the wind field and issue subjective 30-, 50-, and 100-kt wind radius nowcasts (warning time wind field) and 24-, 48-, and 72-hr forecasts.

The wind radius data used in the present study were extracted from a total of 5756 JTWC tropical cyclone warnings issued during the period 1966-77. A typical warning is shown in Fig. 1a.

a.

WESTPAC TROPICAL CYCLONE WARNING

0 151156Z SEP 77 7PU
FM FLENUMCEN GUAM
TO TYPHOON WARNING WESTPAC
INFO/ADMS FUCHU AS JA
ST
UNCLAS //NO3145//
NMA FOR ZKZK PP LTZ DE
WTPA 20 PGTW 151200
TYPHOON JUDY WRNG NR 11
POSIT 31.1N/5 144.8E/7 AT 151200Z
ACCURATE WITHIN 15 NM
BASED ON EYE FIXED AT 30.8N/1 144.6E/5
AT 150942Z BY SATELLITE
CENTER MOVING TOWARD THE NORTHEAST AT 08 KTS
FOR THE NEXT 12 HOURS.
PRESENT WIND DISTRIBUTION
MAX SUSTAINED WINDS 75 KTS NEAR CENTER WITH GUSTS TO 90 KTS
➤ RADIUS OF OVER 50 KT WINDS 75NM
➤ RADIUS OF OVER 30 KT WINDS 175NM SOUTHEAST SEMICIRCLE; 130NM ELSW
REPEAT POSIT 31.1N/5 144.8E/7 AT 151200Z
FORECASTS
12 HRS VALID 160000Z 32.1N/6 146.3E/4
MAX WINDS 70 KTS WITH GUSTS TO 85 KTS
➤ RADIUS OF OVER 50 KT WINDS 70NM SOUTHEAST SEMICIRCLE; 45NM ELSW
24 HRS VALID 161200Z 32.7N/2 148.5E/8
MAX WINDS 60 KTS WITH GUSTS TO 75 KTS
➤ RADIUS OF OVER 50 KT WINDS 45NM SOUTH SEMICIRCLE; 20NM ELSW
➤ RADIUS OF OVER 30 KT WINDS 150NM SOUTH SEMICIRCLE; 100NM ELSW
BECOMING EXTRATROPICAL
EXTENDED OUTLOOK
42 HRS VALID 170600Z 33.3N/9 152.9E/7
MAX WINDS 45 KTS WITH GUSTS TO 55 KTS
EXTRATROPICAL
ACFT RECON PLANNED FOR 151530Z, and 160330Z
NEXT WARNINGS AT 151800Z, 160000Z, 160600Z, AND 161200Z
REMARKS: SATELLITE DATA AT 151003Z ALSO INDICATES
JUDY'S NORTHEASTWARD TRACK.
BT

b.

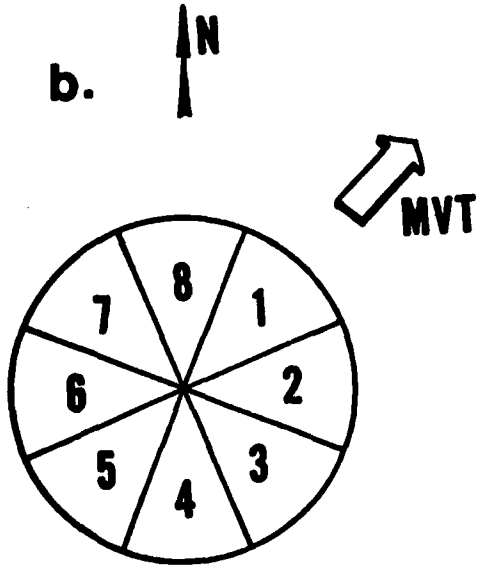

OCTANT	WIND RADIUS (n mi) 50 KT	30 KT
1	75	175
2	75	175
3	75	175
4	75	175
5	75	130
6	75	130
7	75	130
8	75	130

Fig. 1. Examples of (a) typical tropical cyclone warning for the western North Pacific and (b) octant radii of 50 and 30 kt winds extracted from the warning.

For purposes of the asymmetry study, the wind radius is broken into the eight octant components shown in Fig. 1b. The first octant is bisected by the direction of the movement of the storm; the other seven octants rotate clockwise around the center. Given the description of the warning, the wind radius values are always filled from the first octant to eighth. Since the description does not always coincide with the octant angle limits, however, some shifting and truncating are necessary. The larger wind radius report is always decomposed first, and a rounded off operation toward the first octant is applied whenever necessary. Fig. 1b shows the decomposition and the shift of the 175 n mi semicircle of the 30-kt wind radius. Storm position and movement data are extracted from JTWC's Best Track file, which is a data set containing subjectively smoothed paths of tropical cyclones produced by post-analysis of each storm. Best Track positions are used here instead of actual warning time positions because the Best Track file maintains a good continuity of position reports that provides a consistent and logical record of storm direction and speed.

Three characteristics of the data set should be mentioned here, in view of the nature of the data source and the decomposition procedure; these characteristics actually will dictate the course of this study.

(1) A sensitivity analysis comparing the five tropical cyclone warnings with actual ship surface wind reports was conducted for this study, and no significant systematic bias either overestimating

or underestimating wind radius reports was found. Although individual estimates may not be as accurate as desired, the average value or the mean value of 5756 warning reports should still hold true.

(2) The third and the seventh octant wind radii, which correspond to the right hand side (RHS) and left hand side (LHS) wind radii of the storm, are the most reliable estimates; note that these radii were indicated in the warnings (Fig. 1).

(3) It is probable that some of the symmetric tropical cyclones in the data set were actually asymmetric cyclones. In these cases, it is probable that only the largest (or the RHS) wind radius was reported.

3. SURFACE WIND DISTRIBUTION

3.1 Azimuthal Wind Distribution

One of the purposes of this study is to examine the asymmetric nature of a typical tropical cyclone. As discussed by George and Gray (1976) and Frank and Gray (1980), the symmetric pressure perturbation of a tropical cyclone imposed upon a large-scale pressure gradient results in an asymmetric wind distribution around a tropical cyclone. They showed that the wind at the RHS (right hand side) of the storm is indeed greater than the wind at the LHS (left hand side). The asymmetry ($A \equiv r_L/r_R$), which is defined as the ratio of the wind radius at the LHS (r_L) to that of the RHS (r_R), was significantly different from unity in the area about 120 to 240 n mi from the center. To Navy users, though the asymmetry of the tropical cyclone is important, the asymmetric shape of the

entire storm is just as important. For example, ship routing for the purpose of storm evasion requires the information of the wind at specified locations around a tropical cyclone.

In considering a typical asymmetric shape of a tropical cyclone, the first obstacle to be overcome is the scaling of the storms, since the size of a tropical cyclone or the extension of the 50 kt and 30 kt wind radii varies drastically from case to case. To standardize the size distribution in this study, the radius at the RHS of the tropical cyclone is said to be one, and the seven other radius components are made to be fractions of the RHS radius. Of the entire 12-year data set, the mean for the asymmetry of the 50-kt (30-kt) wind radius (Fig. 2) is 0.73 (0.84) with standard deviation of 0.14 (0.15).

The comparisons of the other octant radii with respect to the radius at RHS are also shown in Fig. 2. It is encouraging to find that the mean wind radii for different speeds are all asymmetric and confined in a smooth circle. It is reasonable, therefore, to approximate the shape of the surface horizontal wind distribution as a function of the azimuthal angle (θ), such as,

$$A_\theta \equiv r_\theta / r_R = 1 - (1-A)\,[1 + \cos(\theta - 270)]/2, \qquad (2)$$

where θ is the angle in degrees measured clockwisely from the direction of the storm movement, and A_θ is the asymmetry at azimuthal angle θ, and is defined as the ratio of the radius at θ (r_θ) to the radius at RHS (r_R) of the tropical cyclone. As a result of this expression, which conveniently but realistically assumes a sinusoidal variation of asymmetry around the center, the complex asymmetry

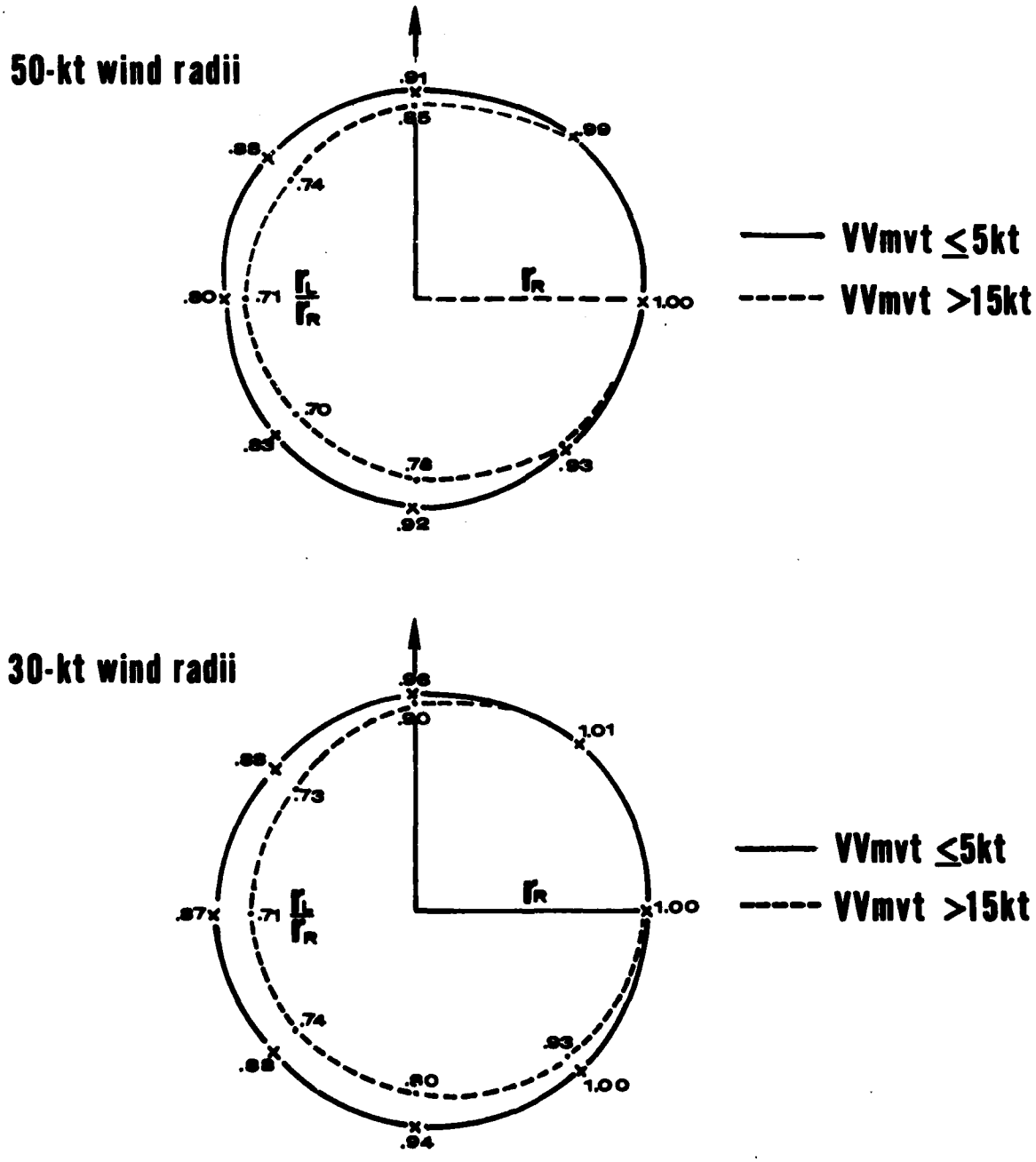

Fig. 2. Average asymmetry of all eight octant wind radii as a function of the speed of movement.

problem is significantly simplified. If the above expression is used in real time, the extent of wind radius around the center of a storm can be deduced from just one observed asymmetry.

An examination of the asymmetry shows that the asymmetry does not vary significantly with the maximum wind, direction of movement, location, and season of the tropical cyclone, but rather that it responds to the speed of the storm's movement: the faster the storm moves, the greater the asymmetry becomes. The correlation between the asymmetry and the speed of the movement (VV_{mvt}) is estimated from the average asymmetries of 1 kt class intervals of the VV_{mvt}. The sample size of each speed class ranges from 29 to 336 cases. There are 19 classes for 30-kt wind radius asymmetries and 18 classes for 50-kt asymmetries. The regression equation for the 50-kt wind radius asymmetry (A_{50}) estimated from the average values of the classes is,

$$A_{50} = rL/rR = 0.863 - 0.005\ VV_{mvt}, \qquad (3)$$

and for 30-kt wind radius asymmetry (A_{30}) is

$$A_{30} = rL/rR = 0.904 - 0.007\ VV_{mvt}, \qquad (4)$$

where VV_{mvt} is measured in kt. The Student t test value for regression Eq. (3) is 41.48. The Student t value at 0.05 significance level ($t_{.05}$) is 4.45 for 17 degrees of freedom (df). The t value for Eq. (4) is 28.94 ($t_{.05} = 4.41$; df = 18). These regression coefficients were tested through a 10-time jackknife procedure, and the results did not vary significantly.

3.2 Radial Wind Profile

Since the azimuthal winds can be estimated by Eq. (2), the entire wind distribution around a tropical cyclone can be estimated, if a referent wind distribution profile along a radius is known. The third octant radial wind profile is selected as the reference profile for two reasons: (1) the third octant is the most data rich octant since the wind radius at the RHS of the cyclone is nearly always reported; and (2) even when the asymmetric storms are reported as symmetric storms, the reported wind radius usually is the largest radius; hence, the RHS radius data should be the most reliable in comparison with the data in the other octants. In the following discussion, if not otherwise specified, the radius, r, refers to the radius at the RHS of the tropical cyclone.

Estimating the radial wind profile at the RHS of the storm is not as straightforward as it seems. Of course, it would be most desirable if wind reports were evenly distributed along a radius, i.e., the wind radii reports were made at various wind speeds. However, for the above described data set, this was not the case. Though the data set contains over 5700 reports, each report consists of only two data points, namely the wind radii of over 30 (r_{30}) and 50 kt (r_{50}). (The wind radius of over 100 kt is rarely reported.) A data compositing technique used here to circumvent this awkwardness utilized a scaled wind speed, V/V_{max}, which, by definition, ranged from 0 to 1. The wind speed (V), of course, had only the two values of 30 and 50 in this data set. Fig. 3a illustrates the conversion of a report for V_{max} = 90 kt, r_{50} = 100 n mi, and r_{30} = 300 n mi.

After all wind radius reports are converted into scalar winds, a new data set consisting of RHS radii and their corresponding scalar wind speeds is formed.

Fig. 3b and Table 1 show the average radii, $\bar{r}$, and their standard deviations, σ, of all scalar wind speeds found in the data set. If the number of data points is less than 30, the $\bar{r}$ is not computed and is not listed or plotted. The exponential curve in Fig. 3b is the plot of,

$$V/V_{max} = e^{\beta(\bar{r}-15)}, \qquad (5)$$

where $\beta = -0.00511$, which was obtained through the least-squares fit of the 32 average radii shown in Table 1. The constant 15 in Eq. (5) is prescribed average radius of the maximum wind in n mi. The Student t test for the β was 6.06 ($t_{.05}$ for df = 29 is 2.05). Since two boundary conditions ($V = V_{max}$ and $V = 0$) are used, only 29 instead of (32-1) degrees of freedom are counted. From Fig. 3b, it seems that the radial wind profile around a tropical cyclone comfortably assumes an exponential profile. Fig. 4 shows the comparison between Eq. (5) and the typical radial wind profile of western North Pacific typhoons compiled by G. Bell (Tse, 1972), Royal Observatory, Hong Kong. The $V_r^{0.55}$ and $V_r^{0.33}$ curves are also plotted in Fig. 4 to delineate the shapes of the V_r^{α} family. To standardize the comparison, the maximum wind used is 92 kt and the radius of the maximum wind (r_{vmax}) is 20 n mi. Both values are extracted from the compilation by Bell. As shown in Fig. 4, the exponential curve is very similar to the curve compiled by Bell;

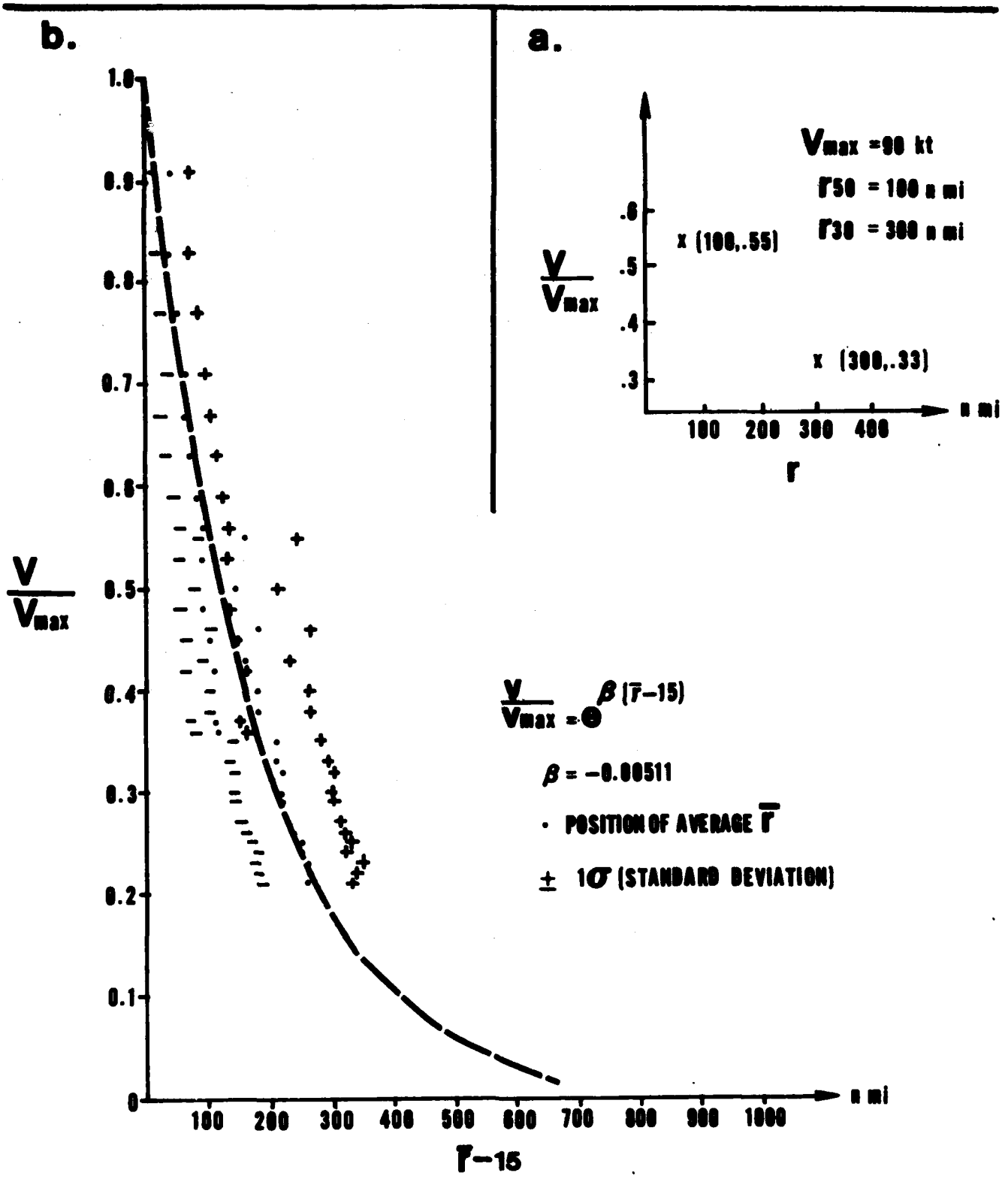

Fig. 3. The inset figure (a) illustrates scaling of wind radii and the larger figure (b) shows the least-squares fit of the average radii. The distance ($\bar{r}$ - 15) is the radial distance from the radius of maximum wind; the constant 15 n mi is a prescribed average radius of maximum wind.

Table 1. Stratified average wind radius, $\bar{r}$, and its standard deviation. Stratification is made according to the scalar wind speed, V/V_{max}. The column No. Obs. shows sample size of each stratified class.

Class Number	V/Vmax	No. Obs.	$\bar{r}$ (n mi)	σ(n mi)
1	.91	273	40	25.9
2	.83	425	40	30.6
3	.77	424	50	33.4
4	.71	325	60	34.7
5	.67	319	60	38.7
6	.63	281	70	38.8
7	.59	258	80	39.1
8	.56	234	90	44.1
9	.55	415	160	78.8
10	.53	166	90	40.4
11	.50	715	140	71.9
12	.48	130	90	43.9
13	.46	462	180	75.8
14	.45	115	100	42.5
15	.43	431	160	73.5
16	.42	96	110	47.1
17	.40	392	180	76.1
18	.38	366	180	78.6
19	.37	32	110	38.0
20	.36	45	120	42.0
21	.35	259	210	74.6
22	.33	261	210	80.1
23	.32	171	220	75.1
24	.30	202	220	75.3
25	.29	133	220	78.4
26	.27	115	230	81.0
27	.26	97	240	80.8
28	.25	96	250	76.7
29	.24	68	250	69.9
30	.23	84	260	87.5
31	.22	32	260	83.1
32	.21	57	260	68.4

however, it deviates from the v-r curves in the area close to the center of the cyclone, where the $Vr^{0.55}$ and the $Vr^{0.33}$ curves tend to confine the high winds near the center. The validity of the deviations at the lower ($V/V_{max}<0.2$) part of Fig. 4 is difficult to assess since the wind speeds are approaching the environmental winds. Holland's (1980) radial profile for a tropical cyclone, used in conjunction with climatological parameters, is very similar to the $Vr^{0.55}$ curve.

Once the winds are scaled, the radius also must be scaled. With two radius reports in each observation, however, the wind radius of a tropical cyclone is rather difficult to scale. Riehl (1963) argued that the r_{vmax}, the radius of maximum wind, should be used as the scaling radius. In this study, however, r_{vmax} could not be treated as a practical referent radius for two reasons: first, r_{vmax} is seldom reported because the shape and size of the eye are often obscured by cloud cover; and second, the r_{vmax} usually ranges from 10 to 30 n mi, so a 5 n mi error in the estimation can lead to a 15-50% error in scaling. Obviously, it is not desirable to use such an estimator as a referent radius for scaling in the operational environment. To avoid the inherent errors in r_{vmax}, the $r_{1/2}$ (the radius where the wind is half of the maximum wind), which equals 150 n mi (truncated from 154 n mi) estimated from Eq. (5), was chosen as the referent radius. Using the scalar radius $(r-15)/(r_{1/2}-15)$, Eq. (5) becomes

$$V/V_{max} = e^{\gamma R/R_{1/2}}, \qquad (6)$$

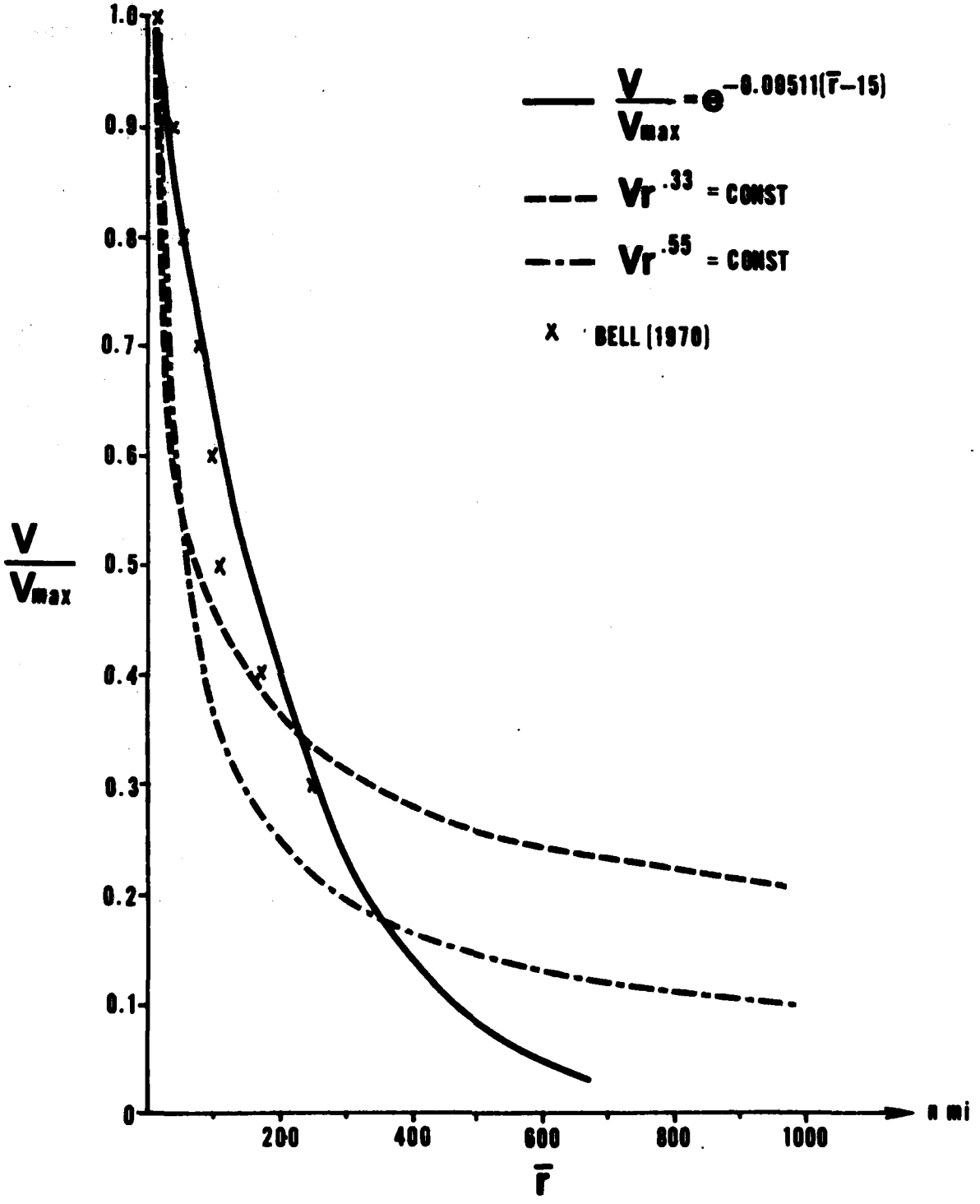

Fig. 4. Radial wind profile comparison. To standardize the comparison, the maximum wind is 92 kt and the radius of the maximum wind is 20 n mi; both values are extracted from Bell's compilation.

where R and $R_{1/2}$ are the radial distances from the maximum wind and $\gamma = -0.00511(150-15)$. To check the validity of Eq. (6), γ is re-estimated by using monthly data. Through the least-squares fit, the estimated γ values varied from -0.638 in April to -0.722 in September, and to 0.658 in November. Evidently, there is a very small seasonal variation which peaks in late summer. For the sake of consistency and simplicity for operational consideration, the γ in Eq. (6) is set to -0.693 so that when $R = R_{1/2}$, V is exactly half of Vmax.

It should be stressed here that the exponential curve of Eq. (6) is deduced from the average radii, not from the warning reports, because:

(1) Wind reports used in this study are not derived from measurements, but from estimates of the true value. With as many estimates as are shown in Table 1, it is believed that the central limit theory would apply, i.e., the averaged value of a sample approaches the true mean.

(2) To examine the average radii is consistent with the purpose of this study, which is to produce a typical radial wind profile for the typical western North Pacific tropical cyclone.

An example of the application of Eqs. (2) and (6) is illustrated in Fig. 5.* The low level (900 mb) wind field (light wind barbs in the figure) of 1977 Hurricane Anita was derived from two GOES-E images 7 1/2 min apart (Rogers et al., 1979). The heavy wind barbs to the north of the center of Anita which is the RHS of this

*Step-by-step computations of the wind radii are demonstrated in the appendix (p. 37).

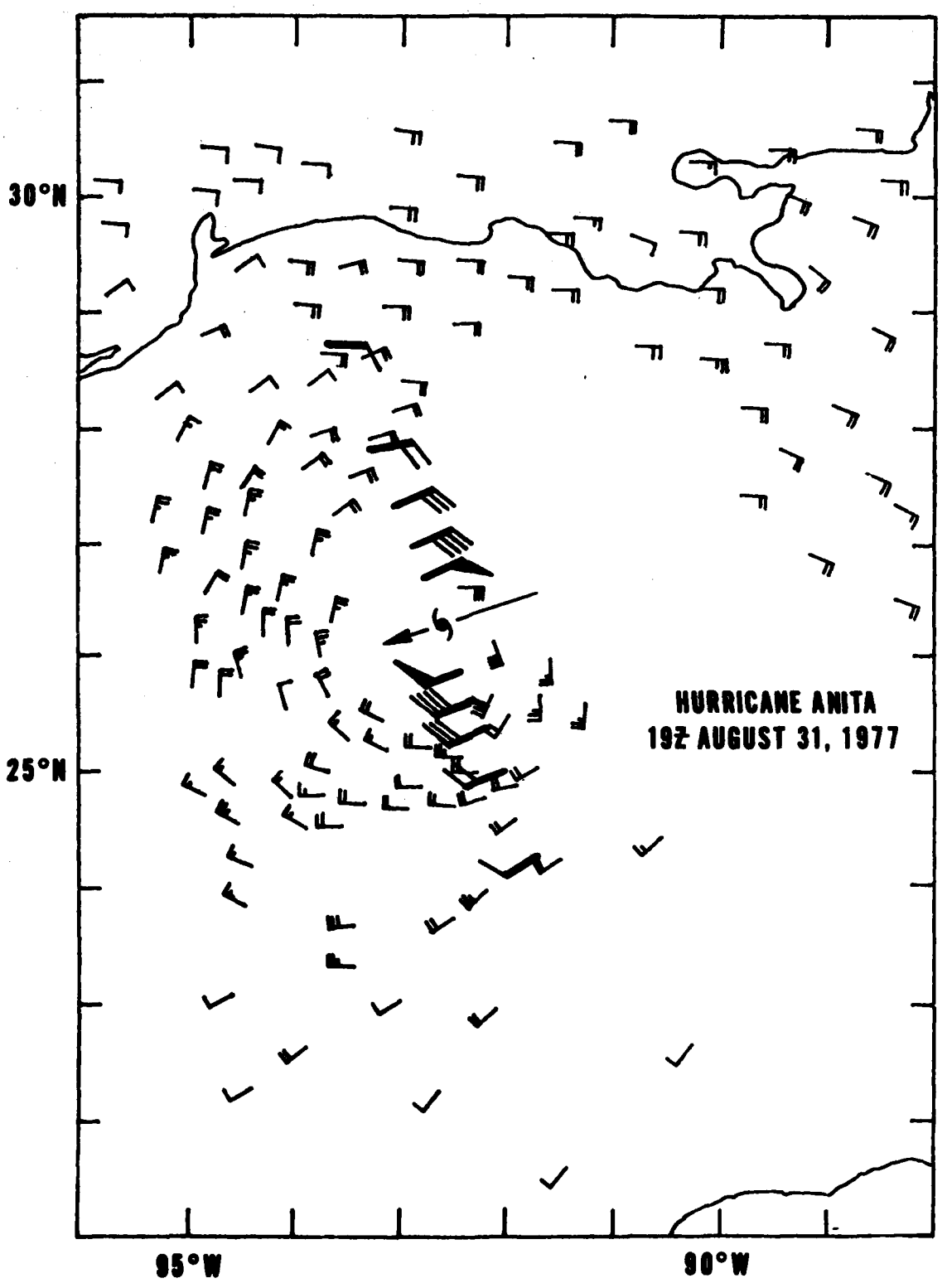

Fig. 5. Low-level winds (light barbs) around Hurricane Anita, generated from two satellite images 7.5 min apart; and winds (heavy barbs) estimated from Eqs. (2) and (6). Units are in ms^{-1}.

hurricane, are estimated from Eqs. (2), (3), and (6) by using the 40 ms^{-1} winds located southeast of the center and using the best track V_{max} (70 ms^{-1}) as inputs. The heavy wind barbs to the south of the center are estimated through Eqs. (2), (3), and (4) by using the climatological asymmetries. It is a simple task to fill in the winds in any other direction not shown in Fig. 5 by changing the azimuthal angle in Eq. (2). It is evident that the winds within the circulation of Hurricane Anita are adequately estimated.

Hence, it is reasonable to conclude that: (1) the winds around a tropical cyclone are exponentially distributed along a radial axis from the radius of maximum wind; (2) the size of a cyclone is highly correlated with the maximum wind; and (3) the shape of a cyclone depends on its speed of movement.

4. WIND RADIUS FORECAST

Another purpose of this study is to produce a simple operational wind radius forecast program which can aid JTWC in the development of tropical cyclone wind radius forecasts. Given the diagnosis of surface wind distribution discussed earlier, it is obvious that maximum wind forecasts should be strong predictors for wind radius forecasts. To ensure that this relationship does not arise because of the particular diagnostic approach utilized, a traditional approach should be used in the derivation of the wind radius forecast algorithm.

To correlate statistically the variation of RHS wind radius (Y) as the predictand to the variation of the other meteorological variables ($x_1, x_2, \ldots x_p$) as the predictors, one can assume that,

$$Y = \sum_i \sum_j a_{ij} x_i^j \; ; \; i = 0,1,2 \ldots p, \text{ and } j = 0,1,2 \ldots, \quad (7)$$

where p is the number of meteorological variables and a_{ij} is the regression coefficient of i^{th} meteorological variable at j^{th} power. Of course, for physical reasons and computational constraints, j usually is no more than 2.

Though this assumption is reasonable and realistic, it has two practical obstacles if the JTWC data set is used. First, it is difficult to know the power relationship between a particular predictor and the predictand, so the initial regression function is difficult to construct. Second, this assumption makes the physical evaluation of the regression coefficients difficult because of the difference in the units and dimensions from one predictor to another. However, an alternative regression function can be used here assuming the correlation exists between the explicit change of the predictand and the predictors. The function can be expressed as

$$\Delta Y/Y = b_0 + \sum_i b_i \, \Delta X_i/X_i + \varepsilon \; ; \; i = 1,2, \ldots p, \qquad (8)$$

where ΔX and ΔY are the changes of X and Y in time, the b_i's are the estimated constant regression coefficients, and ε is the residual. Actually, Eq. (8) is a portion of the result of differentiating Eq. (7) in the logarithmic form without the cross-correlation terms. In concept, Eq. (8) can be interpreted as the percent change of the RHS wind radius ($\Delta Y/Y$) equals the sum of the percent changes of the meteorological variables.

The predictors of Eq. (8) shown in Table 2 include the change of wind radius (persistence), maximum wind (intensity), position (latitude and longitude), and the movement (east-west and north-south components) for the past 6-, 12-, 18-, and 24-hr periods. The

Table 2. Meteorological variables used in Eq. (8). The subscript denotes the time period which is calculated from the warning time (00). Forecast (fcst) periods are +12 and +24 hr.

PREDICTAND:		
1	$R(fcst, 00) = (R_{fcst} - R_{00})/R_{00} * 100\%$	Percent radius change from fcst time to 00 hour.
PREDICTORS:		
1	$R(00, -6) = (R_{00} - R_{-6})/R_{-6} * 100\%$	Percent radius change for the past 6 hours.
2	$R(00, -12) = (R_{00} - R_{-12})/R_{-12} * 100\%$	Percent radius change for the past 12 hours.
3	$R(00, -18) = (R_{00} - R_{-18})/R_{-18} * 100\%$	Percent radius change for the past 18 hours.
4	$R(00, -24) = (R_{00} - R_{-24})/R_{-24} * 100\%$	Percent radius change for the past 24 hours.
5	$I(fcst, 00) = (I_{fcst} - I_{00})/I_{00} * 100\%$	Percent maximum wind (intensity) change from fcst time to 00 hour.
6	$I(00, -6) = (I_{00} - I_{-6})/I_{-6} * 100\%$	Percent maximum wind change for the past 6 hours.
7	$I(00, -12) = (I_{00} - I_{-12})/I_{-12} * 100\%$	Percent maximum wind change for the past 12 hours.
8	$I(00, -18) = (I_{00} - I_{-18})/I_{-18} * 100\%$	Percent maximum wind change for the past 18 hours.
9	$I(00, -24) = (I_{00} - I_{-24})/I_{-24} * 100\%$	Percent maximum wind change for the past 24 hours.
10	$\phi(00, -6) = (\phi_{00} - \phi_{-6})/10° * 100\%$	Percent latitude change for the past 6 hours.
11	$\phi(00, -12) = (\phi_{00} - \phi_{-12})/10° * 100\%$	Percent latitude change for the past 12 hours.
12	$\phi(00, -18) = (\phi_{00} - \phi_{-18})/10° * 100\%$	Percent latitude change for the past 18 hours.
13	$\phi(00, -24) = (\phi_{00} - \phi_{-24})/10° * 100\%$	Percent latitude change for the past 24 hours.
14	$\lambda(00, -6) = (\lambda_{00} - \lambda_{-6})/10° * 100\%$	Percent longitude change for the past 6 hours.
15	$\lambda(00, -12) = (\lambda_{00} - \lambda_{-12})/10° * 100\%$	Percent longitude change for the past 12 hours.
16	$\lambda(00, -18) = (\lambda_{00} - \lambda_{-18})/10° * 100\%$	Percent longitude change for the past 18 hours.
17	$\lambda(00, -24) = (\lambda_{00} - \lambda_{-24})/10° * 100\%$	Percent longitude change for the past 24 hours.
18	$U(00, -6) = (U_{00} - U_{-6})/(VVmvt)_{-6} * 100\%$	Percent E-W movement change for the past 6 hours.
19	$U(00, -12) = (U_{00} - U_{-12})/(VVmvt)_{-12} * 100\%$	Percent E-W movement change for the past 12 hours.
20	$U(00, -18) = (U_{00} - U_{-18})/(VVmvt)_{-18} * 100\%$	Percent E-W movement change for the past 18 hours.
21	$U(00, -24) = (U_{00} - U_{-24})/(VVmvt)_{-24} * 100\%$	Percent E-W movement change for the past 24 hours.
22	$V(00, -6) = (V_{00} - V_{-6})/(VVmvt)_{-6} * 100\%$	Percent N-S movement change for the past 6 hours.
23	$V(00, -12) = (V_{00} - V_{-12})/(VVmvt)_{-12} * 100\%$	Percent N-S movement change for the past 12 hours.
24	$V(00, -18) = (V_{00} - V_{-18})/(VVmvt)_{-18} * 100\%$	Percent N-S movement change for the past 18 hours.
25	$V(00, -24) = (V_{00} - V_{-24})/(VVmvt)_{-24} * 100\%$	Percent N-S movement change for the past 24 hours.

Latitude/longitude changes are divided by the scale of the tropical cyclone (10°). Movement changes are divided by the speed of the movement instead of the respective components.

forecast periods are 12 and 24 hr. The 48- and 72-hr forecast period data are not used because of the small sample size.

By using the International Mathematical and Statistical Library's (IMSL 1979) stepwise regression computer routine RLSEP, the identical five predictors for both 12- and 24-hr forecast periods were selected. These are the R(00,-12) and R(00,-24), the persistence predictors which measure the persistence change of the wind radius for the past 12- and 24-hr periods; and the I(fcst,00), I(00,-12), and I(00,-24), the maximum wind predictors which measure the maximum wind changes for the forecast, past 12, and past 24 hr periods. Then by using a random clustering procedure and the IMSL's multiple linear regression routine RLMUL, all b_i values of the selected five predictors are estimated at above 95% confidence level.

The estimated regression coefficients for the 24-hr forecast period are almost identical to those for the 12-hr period shown in Table 3. Since 61% of the variance can be explained by the five predictors selected for the 12-hr forecast period and only 38% of the variance can be explained by the predictors for the 24-hr period, only the 12-hr forecast algorithm will be used. A review of the selected coefficients in Table 3 shows that only two types of variables, persistence and maximum wind change, are selected. This reconfirms the conclusion found in the diagnostic study, i.e., the size of the radius of a tropical cyclone is positively correlated to the change of the maximum wind and is not significantly related to any other variables.

Table 3. Regression coefficients for the wind radius forecast algorithm for the 12 hr forecast period.

	b_0 constant	b_1 R(00,-12)	b_2 R(00,-24)	b_3 I(fcst,00)	b_4 I(00,-12)	b_5 I(00,-24)
Vmax (kt)	Regression Coefficients for 30-kt wind radius forecast					
31-35	22.984	-0.203	-0.029	0.384	1.961	-0.533
36-45	14.735	-0.163	0.001	0.854	0.910	-0.383
46-55	8.868	-0.167	-0.040	0.291	0.947	-0.143
56-65	8.814	-0.143	-0.048	0.444	0.694	-0.108
66-75	6.388	-0.200	-0.076	0.478	0.199	0.164
76-85	6.760	-0.186	-0.088	0.571	0.240	0.068
86-95	4.046	-0.201	-0.099	0.168	0.331	0.108
96-105	2.724	-0.370	-0.112	-0.207	0.560	0.089
106-115	3.050	-0.502	-0.077	-0.503	1.065	-0.128
116-125	4.696	-0.182	-0.158	0.428	0.444	0.009
126-135	7.268	-0.126	-0.232	0.531	-0.198	0.429
$\geq$ 136	9.254	0.051	-0.295	-0.196	0.168	0.313
Vmax (kt)	Regression Coefficients for 50-kt wind radius forecast					
51-55	-20.259	0.122	-0.229	0.496	0.663	0.950
56-65	-11.070	0.001	-0.141	1.084	0.483	0.669
66-75	8.184	-0.043	-0.301	1.117	0.165	0.994
76-85	14.585	-0.310	-0.057	0.508	1.581	-0.221
86-95	11.585	-0.296	-0.087	0.292	1.349	-0.298
96-105	11.495	-0.330	-0.076	0.400	0.972	-0.148
106-115	7.950	-0.263	-0.081	-0.004	0.806	0.148
116-125	3.932	-0.123	-0.157	1.067	-0.633	0.723
126-135	8.221	-0.289	-0.057	1.106	-1.048	0.875
$\geq$ 136	13.029	-0.365	-0.089	0.972	-0.931	0.812

In further examination of the values of those estimated coefficients, a few interesting aspects of the variation of these coefficients can be observed. The magnitudes of the coefficients of the persistence predictors b_1 and b_2 are almost exclusively small and negative, which implies that the wind radius resists change. For example, if the wind radius has increased for the past 12 or 24 hours, the future wind radius is likely to decrease slightly. This phenomenon may be caused by the nature of the data reporting procedure. If wind radius reports are examined with respect to time, the wind radius variations would resemble a stepwise function (Fig. 6). Once a new value is reported, the future forecast radii tend to be kept at the same magnitudes.

It is not surprising to find that the I(fcst,00) is shown to be positively correlated with the wind radius forecast, since this relationship was demonstrated in Section 3. It is somewhat surprising, however, to find that the most dominant predictors for the 30-kt wind radius forecast is I(00,-12) instead of I(fcst,00). It is possible that although the maximum wind near the center varies immediately with the changes of the central pressure of the cyclone, the wind at a distance from the center cannot adjust as fast as the maximum wind. Hence, a lag exists between the change of the maximum wind and that of the wind radius. The fact that the I(00,-6) predictor is not a significant variable implies that the time lag discussed here may not arise artificially from the reporting procedure and is indeed around 12 hr. This time lag seems to support the idea that the wind-pressure gradient adjustments may

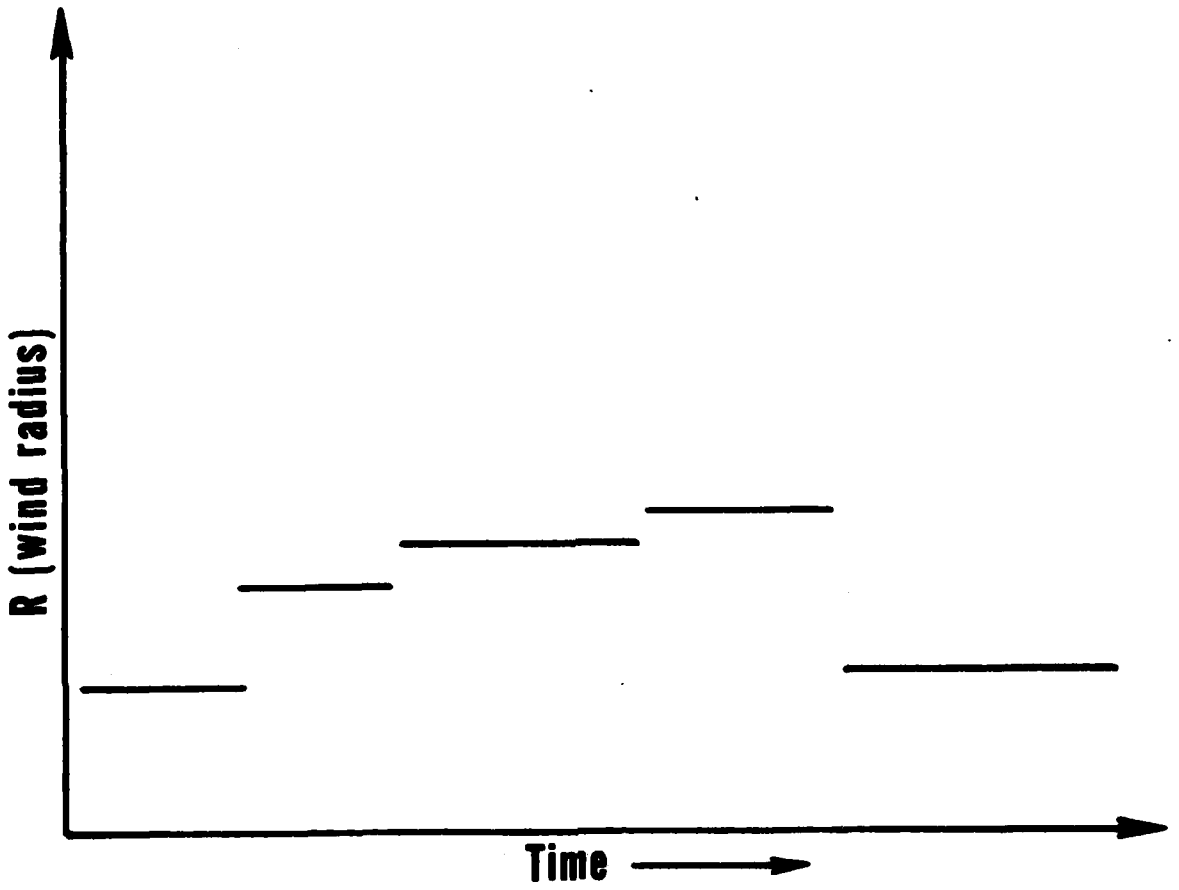

Fig. 6. Schematic diagram of how a wind radius report varies with time.

originate at the inner core of the cyclone and propagate outward. Hence, the wind radius closer to the center would be influenced by changes in intensity before the outer wind radii would change.

With the aid of the regression coefficients shown in Table 3 and the given forecast maximum wind (I_{fcst}), one can estimate the forecast 50 and 30 kt RHS radii (R_{fcst}) by,

$$R_{fcst} = R_{00} \{1 + [b_0 + b_1*R(00,-12) + b_2*R(00,-24) + b_3*I(fcst,00) + b_4*I(00,-12) + b_5*I(00,-24)]/100\}. \quad (9)$$

Once the R_{fcst} from Eq. (9) and the asymmetry from the observation are obtained, the asymmetric surface wind distribution can be estimated from Eq. (2). This wind field then can be adjusted by the actual radius of the maximum wind. If the current maximum wind is equal to or less than 50 kt and is forecast to increase above 55 kt, the RHS 50-kt wind radius can be estimated through Eq. (6) by using the known 30-kt wind radius. In addition, if the RHS 100-kt wind radius is needed, it can be also estimated through Eq. (6) by using the known 50-kt wind radius.

The above described wind radius forecast algorithm has been made into a wind radius forecast aid computer program called WINDIS which currently resides on the computer system at the Fleet Numerical Oceanography Center (FNOC), Monterey, CA, 93940. The WINDIS can be executed via the Naval Environmental Data Network (NEDN) by ARQ number Q92-54--. The exact input/output format for the computer program is described in the Tropical Cyclone Wind

Radius Distribution Program (WINDIS) Functional Description and User's Guide (Tsui, 1980a,b). A sample output of the WINDIS program is shown in Table 4.

A suggested wind radius warning message as part of the WINDIS output is extracted from the results obtained through the above described forecast procedure. These messages are so worded that they can be inserted directly into the Tropical Cyclone Warnings. Forecasters also can select the information from the detailed forecasts as shown in Table 4 to construct a modified wind radius warning message.

The wind radius forecast algorithm (WINDIS) was tested by using 1979 JTWC official tropical cyclone warnings as an independent data set. Since 12-hr, 30-kt wind radius forecasts are not issued, the comparison is made to the 24-hr, 30-kt wind radius forecasts, which are made by doubling the 12-hr forecast procedure. Fig. 7 shows the comparison between the 24-hr, 30-kt radius forecasts made by JTWC and by WINDIS. The R_{OBS} shown in Fig. 7 is the wind radius report at the warning time. Both forecasts are based on the JTWC's maximum wind forecasts so that the comparison will be realistic and homogeneous. To avoid the inherent size difference from cyclone to cyclone, the comparison is made on the deviations from the verified radius: $R_{JTWC} - R_{OBS}$ and $R_{WINDIS} - R_{OBS}$. It is easy to visualize from Fig. 7 that an almost one-to-one positive correlation exists between the two variables. When R_{JTWC} is over- or under-forecast, the R_{WINDIS} correspondingly is over- or under-forecast. Using the coordinates shown in Fig. 7, the least squares fitted slope between

Table 4. Example of output of the wind radius forecast algorithm for Typhoon Hope, 06Z 1 Aug 1979. Input values are underlined.

*****WIND RADIUS DISTRIBUTION PROGRAM*****

TROPICAL CYCLONE HOPE STORM NO. 9, YYMMDDHH=79080106

RADIUS OF EYE : 9 NM

RADIUS OF OVER 30 KT WINDS : 240 NM

RADIUS OF OVER 50 KT WINDS : 90 NM

TAU=00, INTENSITY=125 KTS, LAT,LONG = 20.8N, 121.6E

TAU=12, INTENSITY=115 KTS, LAT,LONG = 21.7N, 118.2E

TAU=24, INTENSITY= 85 KTS, LAT,LONG = 22.5N, 113.9E

TAU=48, INTENSITY= 30 KTS, LAT,LONG = 21.7N, 105.4E

*****FORECASTS FOR THE SYMMETRIC WIND RADII*****

TROPICAL CYCLONE HOPE STORM NO. 9, YYMMDDHH = 79080106

RADIUS OF EYE = 9 NM

TAU =	-24	-12	00	12	24	36	48	60	72
INTENSITY (KTS)	105	130	125	115	85	60	30		
100 KT RADIUS (NM)	15	35	30	25					
50 KT RADIUS (NM)	80	100	90	100	65	15			
30 KT RADIUS (NM)	240	240	240	150	120	45			

***** SUGGESTED WIND RADIUS WARNING MESSAGES *****

TAU=00, VALID AT 79080106

RADIUS OF OVER 100 KT WINDS 30 NM

RADIUS OF OVER 50 KT WINDS 90 NM NNN QUAR, 75 NM ELSW

RADIUS OF OVER 30 KT WINDS 240 NM NNN QUAR, 210 NM ELSW

TAU=12, VALID AT 79080118

RADIUS OF OVER 100 KT WINDS 25 NM

RADIUS OF OVER 50 KT WINDS 100 NM NNN QUAR, 80 NM ELSW

RADIUS OF OVER 30 KT WINDS 150 NM NNN QUAR, 130 NM ELSW

TAU= 24, VALID AT 79080206

RADIUS OF OVER 50 KT WINDS 65 NM NNN QUAR, 50 NM ELSW

RADIUS OF OVER 30 KT WINDS 120 NM NNN QUAR, 100 NM ELSW

TAU=48, VALID AT 79080306

NONE

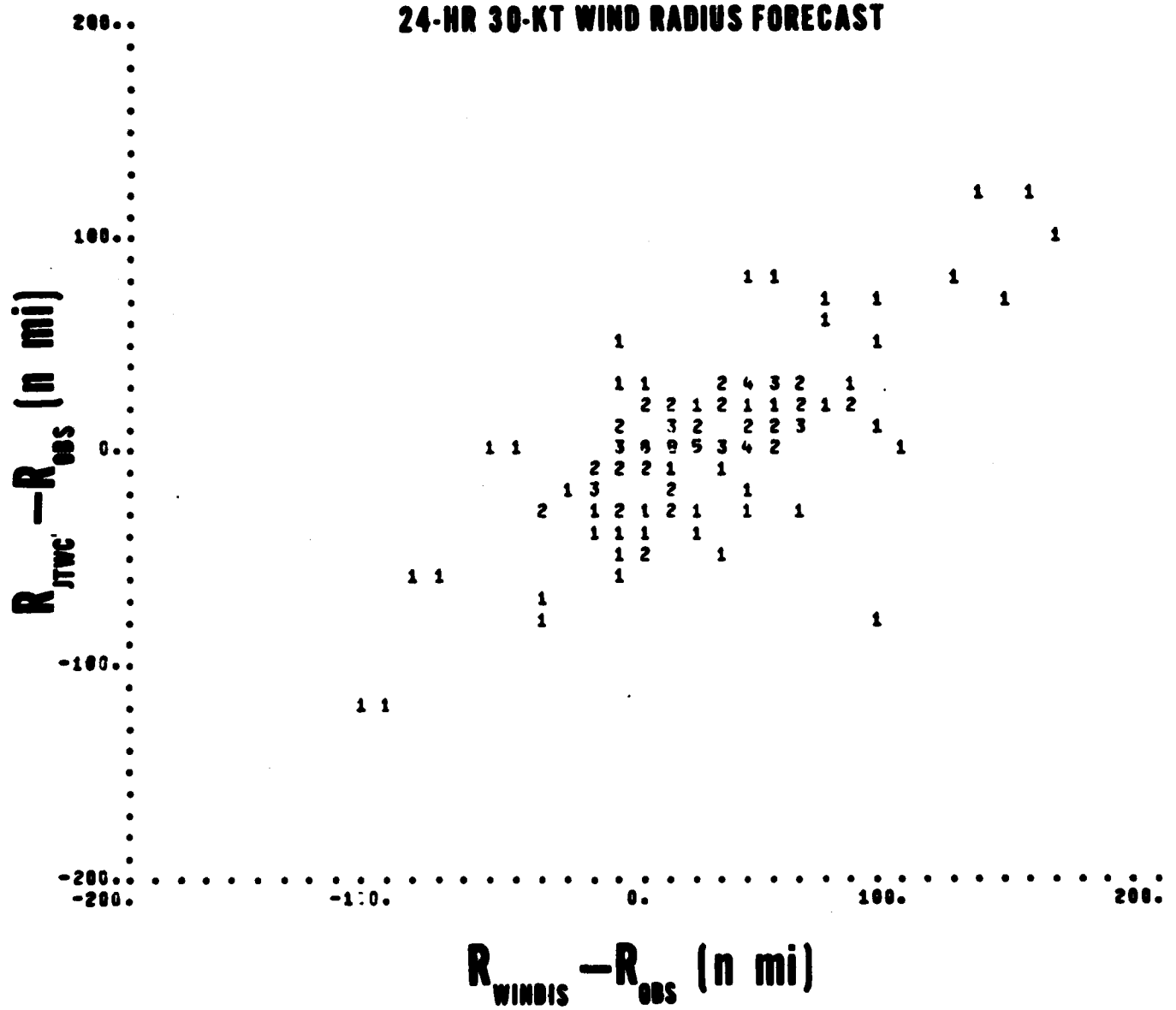

Fig. 7. Comparison of 117 pairs of R_{WINDIS} and R_{JTWC} 24-hr forecasts of 1979 season. Numerals indicate the numbers of data points. Plotting space is limited to a single space by use of alphabets after the numerals; 'A' represents 10 data points, 'B' represents 11 data points, etc.

the two variables is 0.938 (Student t score = 19.6, df = 116). The average error for WINDIS is 37 n mi and 30 n mi for JTWC. For all practical purposes, the WINDIS algorithm possesses skills similar to those of JTWC forecasters. The algorithm, in a sense, actually has quantified the combined experience of all JTWC forecasters and can be very useful for the new forecasters. To produce the wind radius forecasts beyond the 12-hr period, the algorithm is repeated (providing that the forecast maximum winds are given).

Fig. 8 shows a comparison similar to that just discussed, except for the 50-kt wind radius for the 12- and 24-hr forecast periods. The average forecast error of 189 cases for R_{WINDIS} for the 12-hr forecast period is 16 n mi, and for R_{JTWC} is 12 n mi. The average error of 76 cases for R_{WINDIS} for the 24-hr forecast period is 17 n mi and for R_{JTWC} is 14 n mi. It is clear that the trends for both periods are very similar to the trend shown in Fig. 7.

5. SUMMARY

A unique surface 50 kt and 30 kt wind radius data set has been compiled from the tropical cyclone warnings issued by JTWC between 1966 and 1977. The results of two different analysis methods applied to this data set indicate that the change of the size or the wind radius of a typical western North Pacific tropical cyclone depends on the change of the maximum wind. Persistence is also detected in the wind radius variation. In addition, the surface wind exponentially decreases along a radial axis from the maximum wind as the distance from the radius of the maximum wind increases.

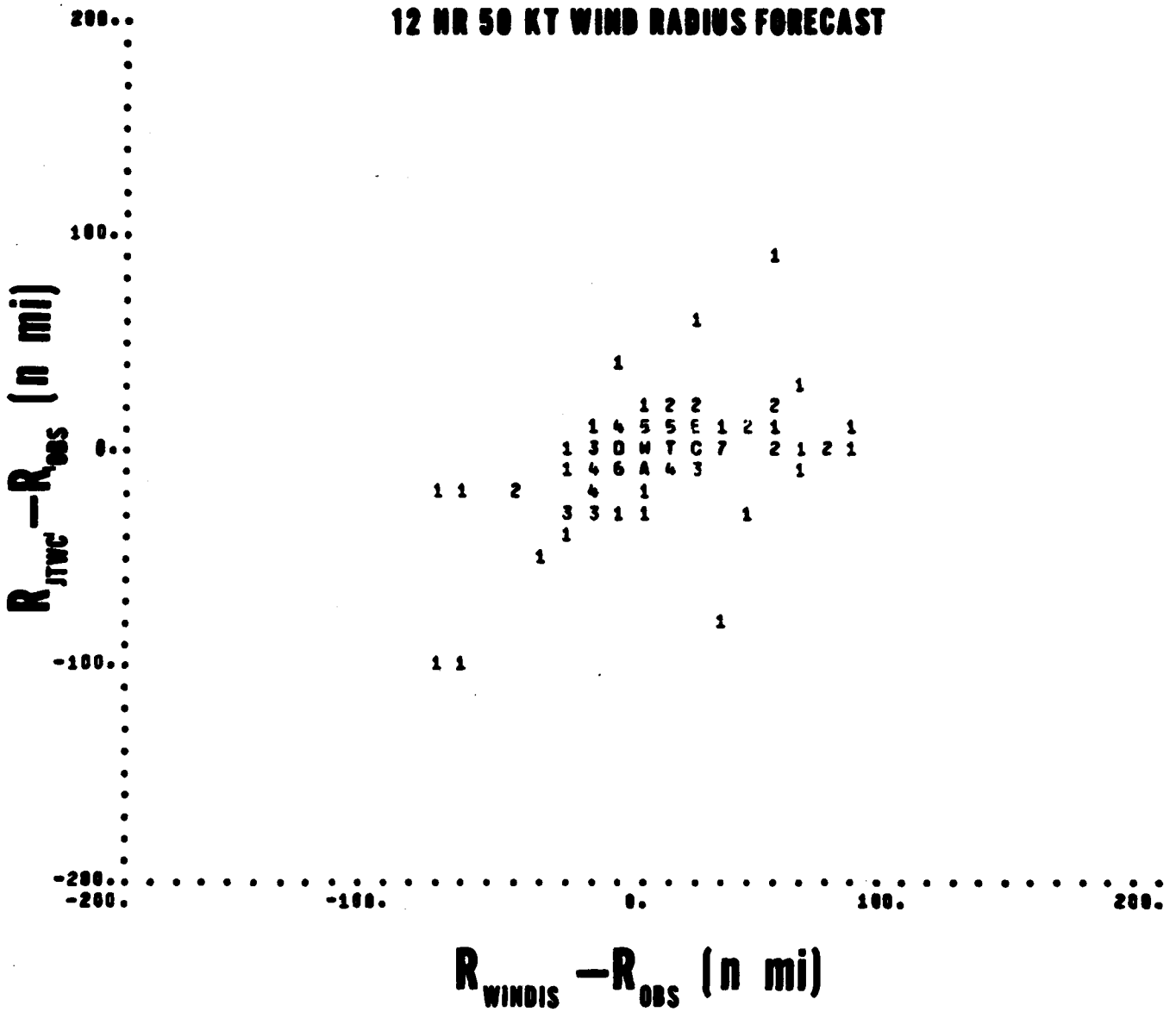

Fig. 8. Similar to Fig. 7, except for comparisons of 189 pairs for the 12 hr 50 kt forecast (this page) and 76 pairs for the 24 hr 50 kt forecast (next page).

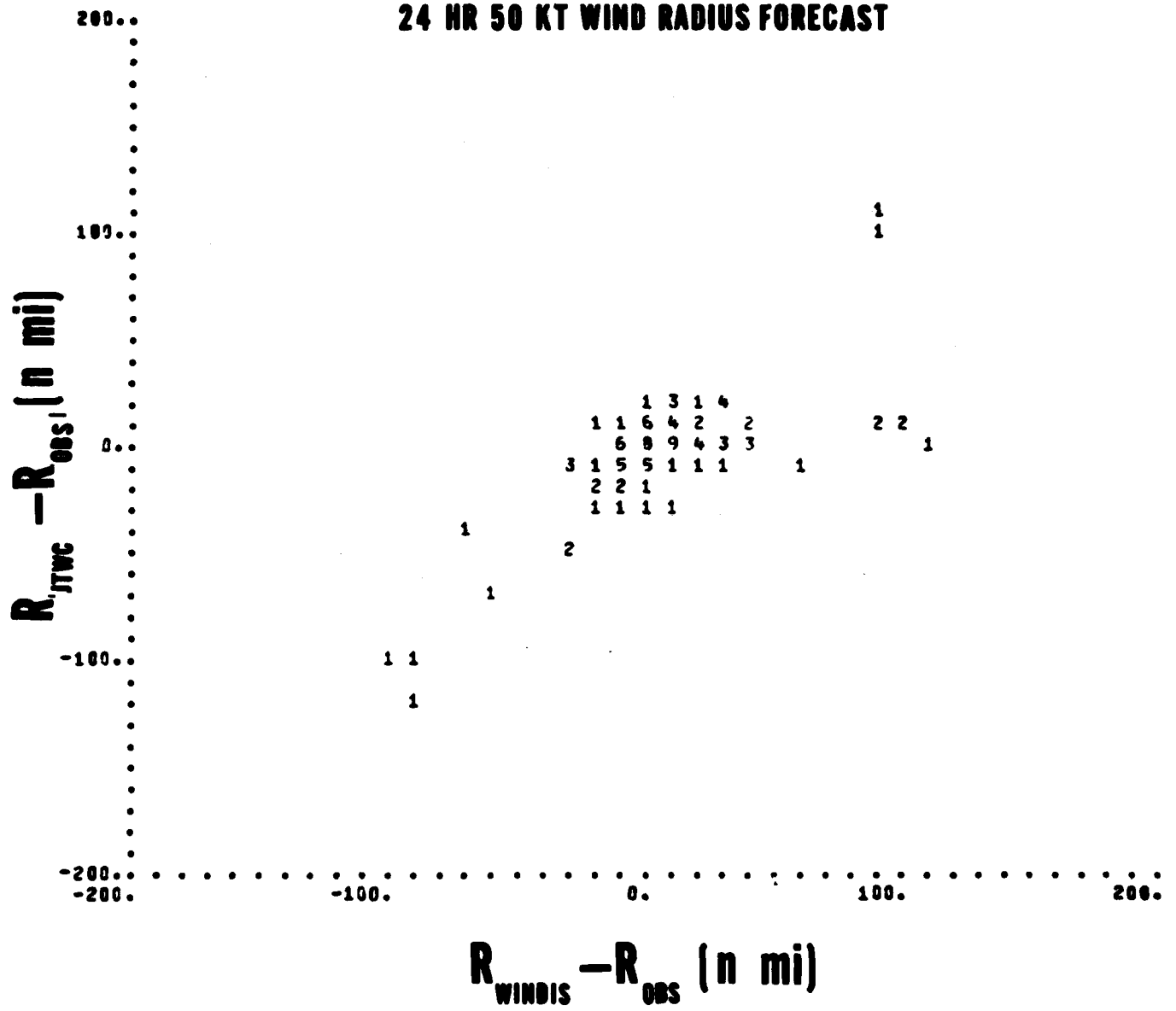

Fig. 8, continued.

The exponential relationship is similar to, but more flexible than, the Vr relationship which has been traditionally thought of as the radial wind profile for a tropical cyclone. Results also show that a time lag exists between the change of the maximum wind and the change of the 30-kt wind radius. This suggests that the wind-pressure gradient adjustments may originate from the inner core of the storm and slowly propagate outward.

Results of the asymmetry study indicates that the asymmetry of the typical western North Pacific tropical cyclone depends on the speed of movement of the cyclone. On the average, the LHS wind radius is 70-80% of the RHS radius.

Also formulated is an empirical wind radius forecast algorithm in which the forecast change of RHS wind radius of a tropical cyclone depends on the past wind radius change, and the past forecast change of the maximum wind. Thus, by providing only the forecast of maximum wind, the RHS forecast wind radii can be estimated via Eq. (9). If these forecast wind radii are incorporated with the radial wind profile, Eq. (6), and the azimuthal wind distribution, Eq. (2), relationships, a typical asymmetric forecast wind distribution around a western North Pacific tropical cyclone can be estimated. For all practical purposes, this empirical wind radius forecast algorithm reflects the combined experience of all JTWC forecasters and exhibits an objective wind radius forecast skills similar to those of a JTWC forecaster.

ACKNOWLEDGMENTS

We are grateful to the Joint Typhoon Warning Center and the Fleet Numerical Oceanography Center for providing the entire archival western North Pacific tropical cyclone warnings.

REFERENCES

Atkinson, G. D., and C. R. Holliday, 1977: Tropical cyclone minimum sea level pressure-maximum sustained wind relationship for western North Pacific, Mon. Wea. Rev., 105, 421-427.

Bates, J., 1977: Vertical shear of the horizontal wind speed in tropical cyclones, NOAA ERL WMPO-39, 19 pp.

Byers, H. R., 1944: General Meteorology, McGraw Hill, N.Y., 417-448.

Deppermann, C. E., 1947: Notes on the origin and structure of Philippine typhoons, Bull. Amer. Meteor. Soc., 28, 399-404.

Dvorak, V. F., 1975: Tropical cyclone intensity analysis and forecasting from satellite imagery, Mon. Wea. Rev., 10, 420-430.

Frank, W. M. and W. M. Gray, 1980: Radius and frequency of 15 ms-1 (30 kt) winds around tropical cyclones, J. Appl. Meteor., 19, 219-223.

George, J. E. and W. M. Gray, 1976: Tropical cyclone motion and surrounding parameter relationships, J. Appl. Meteor., 15, 1252-1264.

Holland, G. J., 1980: An analytic model of the wind and pressure profiles in hurricanes, Mon. Wea. Rev., 108, 1212-1218.

Hughes, L. A., 1952: On the low-level wind structure of tropical storms, J. Meteor., 9, 422-428.

IMSL, 1979: Reference manual of the IMSL Library, 7th ed., IMSL, Houston, Texas 77036.

Riehl, H., 1963: Some relations between wind and thermal structures of steady state hurricanes, J. Atmos. Sci., 20, 276-287.

Rogers, E., R. C. Gentry, W. Shenk, and V. Oliver, 1979: The benefits of using short - internal satellite images to derive winds for tropical cyclones, Mon. Wea. Rev., 107, 575-584.

Shea, D. J. and W. M. Gray, 1973: The hurricane's inner core region - I: symmetric and asymmetric structure, J. Atmos. Sci., 30, 1544-1563.

ieets, R. C., 1978: Hurricane Anita - a new era in airborne research, Mar. Wea. Log., 22, 1-8.

ie, S. Y. W., 1972: The "average" typhoon, WMO No. 321, 82-104.

iui, T. L., 1980a: The tropical cyclone wind radius distribution program (WINDIS) - functional description, NAVENVPREDRSCHFAC 7W0513-FD02.

_____, 1980b: The tropical cyclone wind radius distribution program (WINDIS) - user's manual, NAVENVPREDRSCHFAC 7W0513-UM03.

APPENDIX

EXAMPLE OF ASYMMETRIC WIND DISTRIBUTION COMPUTATION

In the following example, Hurricane Anita's wind distribution at 19Z August 31, 1977 is deduced from the known intensity and one observed wind. As stated in the text, the equations used are

$$A_\theta \equiv r_\theta / rR = 1 - (1-A)\,[1 + \cos(\theta - 270)]/2 \,, \qquad (2)$$

and

$$V/V_{max} = e^{\gamma(R/R1/2)} \,, \qquad (6)$$

where $\gamma = -0.693$.

Input:

1. Intensity of Anita at 19Z August 31, 1977 extracted from Mariners Weather Log (January 1978),

   $V_{max} = 67\ ms^{-1}$.

2. Wind observation extracted from Fig. 5. The 40 ms^{-1} wind at 41 n mi SSE of the center is used in this example.

3. Asymmetry is set at climatological value,

   $A = 0.84$

Computation Steps:

1. Convert the wind observation to the wind at RHS of Anita. By rearranging Eq. (2) and letting

   $\theta = 180^o$,

   $A = 0.84$,

   $r_\theta = 40$ n mi,

   Eq. (2) yields

   $r_R = 50$ n mi

2. Find the referent radius $R_{1/2}$. By rearranging Eq. (6) and letting

$$V = 40 \text{ ms}^{-1},$$

$$V_{max} = 67 \text{ ms}^{-1},$$

$$R = r-15 = 50-15 = 35 \text{ n mi},$$

Eq. (6) yields

$$R_{1/2} = 47 \text{ n mi}$$

3. Now, we have obtained $R_{1/2}$. Since V_{max} is known, Eq. (6) can produce any radius (r) by any given wind (V); e.g.,

$V = 50 \text{ ms}^{-1}$, $R = 19$ n mi, $r = (R+15) = 34$ n mi;

$V = 30 \text{ ms}^{-1}$, $R = 54$ n mi, $r = (R+15) = 69$ n mi;

$V = 20 \text{ ms}^{-1}$, $R = 82$ n mi, $r = (R+15) = 97$ n mi;

$V = 10 \text{ ms}^{-1}$, $R = 129$ n mi, $r = (R+15) = 144$ n mi.

4. Find the wind radii at any arbitrary azimuthal angles. In Fig. (5), the angle of 180^{o} is used. By rearranging Eq. (2) and letting

$$\theta = 180^{o} \ (r_{180} \equiv r_L),$$

$$A = 0.84,$$

then

$r_L = 34$ n mi, if $r_R = 28$ n mi;

$r_L = 69$ n mi, if $r_R = 58$ n mi;

$r_L = 97$ n mi, if $r_R = 81$ n mi;

$r_L = 144$ n mi, if $r_R = 121$ n mi;

DISTRIBUTION LIST

COMTHIRDFLT
CODE N702/01T
PEARL HARBOR, HI 96860

COMSEVENTHFLT
ATTN: NSAP SCI. ADVISOR
BOX 167
FPO SEATTLE 98762

COMNAVAIRPAC
NSAP SCI. ADV. (016)
NAS, NORTH ISLAND
SAN DIEGO, CA 92135

COMNAVSURFPAC
ATTN: NSAP SCI. ADV., 005/N6N
SAN DIEGO, CA 92155

CHIEF OF NAVAL RESEARCH (2)
LIBRARY SERVICES, CODE 734
RM 633, BALLSTON TOWER #1
800 QUINCY ST.
ARLINGTON, VA 22217

OFFICE OF NAVAL RESEARCH
CODE 428AT
ARLINGTON, VA 22217

OFFICE OF NAVAL RESEARCH
CODE 420
ARLINGTON, VA 22217

CHIEF OF NAVAL OPERATIONS
(OP-952)
U.S. NAVAL OBSERVATORY
WASHINGTON, DC 20390

CHIEF, ENV. SVCS. DIV.
OJCS (J-33)
RM. 2877K, THE PENTAGON
WASHINGTON, DC 20301

NAVAL DEPUTY TO THE
ADMINISTRATOR, NOAA
RM. 200, PAGE BLDG. #1
3300 WHITEHAVEN ST. NW
WASHINGTON, DC 20235

OFFICER IN CHARGE
SERVICE SCHOOL COMMAND
DET. CHANUTE/STOP 62
CHANUTE AFB, IL 61868

COMMANDING OFFICER
ATTN: LIBRARY;, CODE 2620
WASHINGTON, DC 20390

OFFICE OF NAVAL RESEARCH
EAST/CENTRAL OFFICE
BLDG. 114, SECT. D
459 SUMMER ST.
BOSTON, MA 02210

COMMANDING OFFICER
NORDA, CODE 101
NSTL STATION
BAY ST. LOUIS, MS 39529

COMNAVOCEANCOM
NSTL STATION
BAY ST. LOUIS, MS 39529

COMMANDING OFFICER
FLENUMOCEANCEN
MONTEREY, CA 93940

COMMANDING OFFICER
NAVWESTOCEANCEN
BOX 113
PEARL HARBOR, HI 96860

COMMANDING OFFICER
U.S. NAVOCEANCOMCEN
BOX 12, COMNAVMARIANAS
FPO SAN FRANCISCO 96630

COMMANDING OFFICER
U.S. NAVOCEANCOMFAC
FPO SEATTLE 98762

SUPERINTENDENT
LIBRARY REPORTS
U.S. NAVAL ACADEMY
ANNAPOLIS, MD 21402

CHAIRMAN
OCEANOGRAPHY DEPT.
U.S. NAVAL ACADEMY
ANNAPOLIS, MD 21402

CHIEF, SCIENTIFIC SERVICE
NWS, PACIFIC REGION
P.O. BOX 50027
HONOLULU, HI 96850

COMMANDER (2)
ATTN: LIBRARY, AIR-00D4
WASHINGTON, DC 20361

COMMANDER
NAVAIRSYSCOM, AIR-333
WASHINGTON, DC 20361

COMMANDER
NAVAIRSYSCOM
MET. SYS. DIV., AIR-553
WASHINGTON, DC 20360

COMMANDER
NAVAIRSYSCOM, AIR-03
NAVY DEPT.
WASHINGTON, DC 20361

DIRECTOR
NAVSURFWEACEN, WHITE OAKS
NAVY SCI. ASSIST. PROGRAM
SILVER SPRING, MD 20910

CHIEF OF NAVAL EDUCATION
& TRAINING
NAVAL AIR STATION
PENSACOLA, FL 32508

NAVAL POSTGRADUATE SCHOOL
METEOROLOGY DEPT. CODE 63
MONTEREY, CA 93940

USAFETAC/TS
SCOTT AFB, IL 62225

3350TH TECH. TRNG GROUP
TTGU/2/STOP 623
CHANUTE AFB, IL 61868

AFGWC/DAPL
OFFUTT AFB, NE 68113

AFGL/LY
HANSCOM AFB, MA 01731

COLORADO STATE UNIVERSITY
ATMOSPHERIC SCIENCES DEPT.
ATTN: LIBRARIAN
FORT COLLINS, CO 80521

COMMANDING OFFICER
U.S. ARMY RSCH OFFICE
ATTN: GEOPHYSICS DIV.
P.O. BOX 12211
RESEARCH TRIANGLE PARK,
NC 27709

DIRECTOR (12)
DEFENSE TECH. INFORMATION
CENTER, CAMERON STATION
ALEXANDRIA, VA 22314

CHIEF
MARINE SCIENCE SECTION
U.S. COAST GUARD ACADEMY
NEW LONDON, CT 06320

ACQUISITIONS SECTION
IRDB-D823, NOAA
LIBRARY & INFO. SERVICE
6009 EXECUTIVE BLVD.
ROCKVILLE, MD 20852

CHIEF, MARINE & EARTH
SCIENCE LIBRARY
NOAA, DEPT. OF COMMERCE
ROCKVILLE, MD 20852

FEDERAL COORDINATOR FOR
METEORO. SERVS. &
SUPP. RSCH. (OFCM)
SUITE 300
11426 ROCKVILLE PIKE
ROCKVILLE, MD 20852

DIRECTOR
NATIONAL HURRICANE CENTER
NOAA, GABLES ONE TOWER
1320 S. DIXIE HWY
CORAL GABLES, FL 33146

NATIONAL CLIMATIC CENTER
ATTN: L. PRESTON D542X2
FEDERAL BLDG. - LIBRARY
ASHEVILLE, NC 28801

COLLEGE OF ARTS & SCIENCES
METEOROLOGY DEPT.
UNIV. OF THE PHILIPPINES
DILMAN, QUEZON CITY 3004
PHILIPPINES

COORDINATOR, NATIONAL ATMOS.
RESEARCH PROGRAM
INSTITUTE OF PHYSICS
ACADEMIA SINICA
TAIPEI, TAIWAN

DIRECTOR, CENTRAL PACIFIC
HURRICANE CENTER
NWS, NOAA
HONOLULU, HI 96819

DIRECTOR, NATIONAL
HURRICANE RSCH LAB (AOML)
1320 S. DIXIE HWY.
CORAL GABLES, FL 33146

DR. E. W. FRIDAY
NATIONAL WEATHER SERVICE
GRAMAX BLDG.
8060 13TH ST.
SILVER SPRING, MD 20910

HEAD, ATMOS. SCI. DIV.
NATIONAL SCI. FOUNDATION
1800 G STREET, NW
WASHINGTON, DC 20550

GODDARD SPACE FLIGHT CEN.
NASA, ATMOS. SCI. LAB.
GREENBELT, MD 20771

EXECUTIVE SECRETARY, CAO
SUBCOMMITTEE ON ATMOS. SCI
NATIONAL SCI. FOUNDATION
RM. 510, 1800 G. ST., NW
WASHINGTON, DC 20550

NATIONAL CENTER FOR ATMOS.
RESEARCH
LIBRARY ACQUISITIONS
P.O. BOX 3000
BOULDER, CO 80302

COLORADO STATE UNIVERSITY
ATMOSPHERIC SCIENCES DEPT.
ATTN: DR. ROGER PIELKE
FORT COLLINS, CO 80523

UNIVERSITY OF HAWAII
METEOROLOGY DEPT.
2525 CORREA ROAD
HONOLULU, HI 96822

TYPHOON RESEARCH LAB.
ATTN: LIBRARIAN
METEORO. RSCH. INSTITUT
1-1 NAGAMINE, YATABE-MACHI
TSUKUBA-GUN
IBARAKI-KEN, 305, JAPAN

CENTRAL WX BUREAU
64, KUNG YUAN RD.
TAIPEI, TAIWAN 100

COLORADO STATE UNIVERSITY
ATMOSPHERIC SCIENCES DEPT.
ATTN: DR. WILLIAM GRAY
FORT COLLINS, CO 80523

THE EXECUTIVE DIRECTOR
AMERICAN METEORO. SOCIETY
45 BEACON ST.
BOSTON, MA 02108

AMERICAN METEORO. SOCIETY
METEO. & GEOASTRO ABSTRACTS
P.O. BOX 1736
WASHINGTON, DC 20013

DIRECTOR, JTWC
BOX 17
FPO SAN FRANCISCO 96630

WORLD METEOROLOGICAL
ORGANIZATION, ATS DIV.
ATTN: N. SUZUKI
CH-1211, GENEVA 20
SWITZERLAND

BUREAU OF METEOROLOGY
ATTN: LIBRARY
BOX 1289K, GPO
MELBOURNE, VIC, 3001
AUSTRALIA

LIBRARY
AUSTRALIAN NUMERICAL
METEORO. RSCH. CENTER
P.O. BOX 5089A
MELBOURNE, VICTORIA, 3001
AUSTRALIA

DIRECTOR
ROYAL OBSERVATORY
NATHAN ROAD, KOWLOON
HONG KONG, B.C.C.

NATIONAL DEFENSE DEPT.
TECHNICAL LIBRARY
WEATHER BUREAU
LUNGSOD NG QUEZON
QUEZON, PHILIPPINES

ATMOSPHERIC SCIENCE DEPT.
NATIONAL TAIWAN UNIVERSITY
TAIPEI, TAIWAN 107